Magnetic Resonance Based Control of a Robotic Manipulator for Interventions in the Beating Heart

Erol Yeniaras, Johann Lamaury, Nikhil Navkar, Dipan J. Shah, Karen Chin, Zhigang Deng, and Nikolaos V. Tsekos

***Abstract*-As a part of an ongoing project, in this paper we introduce the first version of a system which has a novel methodology for Cine (as in cinema) MRI based control of a cardiac robot for beating heart surgeries. The system uses the preoperative planning approach that we developed earlier, and integrates it to the intraoperative algorithms for controlling a robot and tracking some specific landmarks of a highly dynamical surgical field. In particular, our late studies presented herein aim to demonstrate the feasibility of integrating appropriate computational tools to achieve the volumetric image guidance for minimally invasive surgeries in the beating heart. We conceive of the system as practicable for *in vitro* experiments upon the completion of the first physical prototype, which may pave the way for expansion of the approach for other complex surgeries as well.**

I. Introduction

Clinical research in minimally invasive surgeries (MIS) and image guided interventions (IGI) has been evolving toward the development of safer and more cost effective methodologies. Evidently, the major challenge in both planning and performing IGI is the introduction of a viable approach for indirect visualization, which provides the operator a clear and intuitive perception of the surgical field.

Specifically, the MIS in the beating heart (off-pump) can substantially benefit from real-time (RT) image guidance for overcoming the difficulties caused by the cardiac motion, e.g., safe maneuvering of the surgical tools, correct assessment of tissue functionality before and during the surgery [1]. Although the use of robotic devices in cardiac surgeries has been accepted over the last decade, RT image guidance in the absence of direct vision is a relatively new topic which has been investigated by only a few teams [3-6]. One of the well-accepted imaging modalities for RT guidance is three-dimensional (3D) ultrasound due to its volumetric imaging capabilities and lack of ionizing radiation [2, 3], in particular, when robotic systems are used to synchronize the motion of a device with that of the heart [3]. The existing literature in the field of robotic surgeries is vast and inclusive of highly innovative approaches; herein, we only focus on a few most related efforts and it is by no means a comprehensive literature review.

RT magnetic resonance imaging (MRI) is another promising modality for IGI in the heart [4-11]. In addition to volumetric imaging capabilities and the absence of ionizing radiation, MRI provides a better soft-tissue contrast than the other modalities. However, developing an MRI-compatible robotic system is a major challenge due to the strong magnetic fields, the rapidly switching magnetic field gradients, and the narrow space inside the scanners.

In spite of these difficulties, there has been developed a number of MRI-compatible robotic systems [12-14], which resulted in enabling technologies that could contribute to performing MRI guided complex MIS including transapical aortic valve implantations [4-6]. To the best of our knowledge, there is not any clinically approved MRI-guided robotic system for off-pump intracardiac surgeries today.

This paper introduces the design of an intracardiac surgery system that includes necessary computational tools and software modules for creating a realistic visualization of the beating heart based on MRI [15]. Specifically, the contributions of the proposed system are: (1) A methodology for preoperative planning which can be adapted for a broad range of sophisticated surgeries; (2) Showing the feasibility of an MRI-compatible robotic system for surgeries in the beating heart; (3) Providing a user friendly visual environment to the operator for following the operation and adjusting the image acquisition parameter on-the-fly; (4) Assessing the possibility of using MRI as the primary imaging modality for off-pump, robot-assisted aortic valve implantation with transapical approach as shown in Fig. 1.

The system is designed to be a modular platform suitable for further development and testing, both in the laboratory and at the MR suite. The core approach is to define dynamic trajectories and access corridors that

Manuscript received February 8, 2011. This work was supported in part by the National Science Foundation award NSF CNS-0932272. All opinions, findings, conclusions or recommendations expressed in this work are those of the authors and do not necessarily reflect the views of our sponsors.

Erol Yeniaras, Johann Lamaury and Nikolaos V. Tsekos are with the Medical Robotics Laboratory, Department of Computer Science at University of Houston, Houston, TX 77204, USA (phone: 713-743-3350; fax: 713-743-3335; emails: yeniaras@cs.uh.edu, johann.lamaury@gmail.com and ntsekos@cs.uh.edu).

Dipan J. Shah and Karen Chin are with the Methodist DeBakey Heart & Vascular Center, Houston, TX 77030 USA (e-mail: djshah@tmhs.org and KEChin@tmhs.org).

Zhigang Deng and Nikhil Navkar are with the Computer Graphics and Interactive Media Lab. at the Department of Computer Science, University of Houston, Houston, TX 77204 USA (e-mails: zdeng@cs.uh.edu and nnavkar@cs.uh.edu).

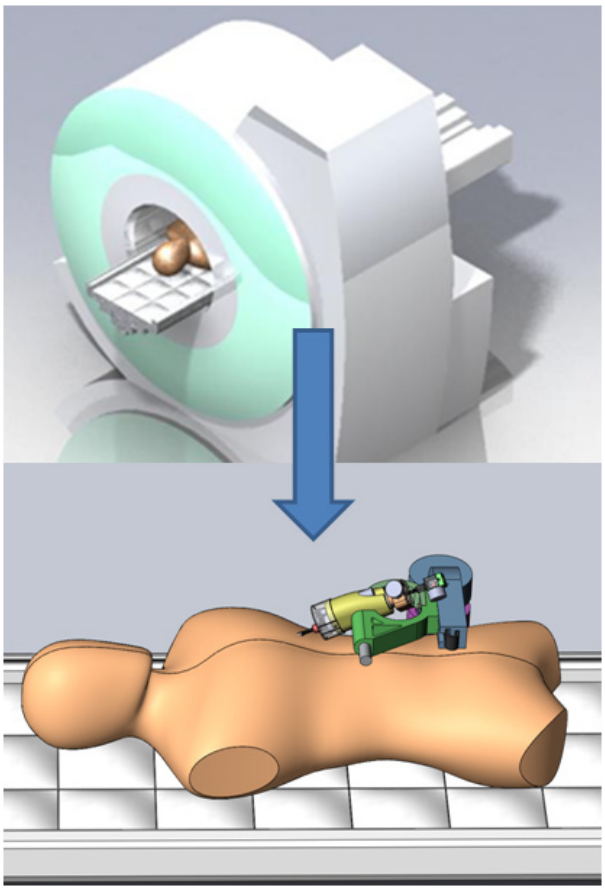

Fig. 1 The conceptual design of the system is depicted: the robotic manipulator enters the heart with a transapical approach inside the MR scanner.

allow appropriate robotic devices to safely transverse the left ventricle (LV) of the heart while it is beating [16]. Dynamic MRI were collected and presented in Cinematic (cine) mode which allows the image acquisition in the form of continuous movies.

While the computational core has the routines to interface to a suitable MR scanner for on-line operation, in this work the system was tested off-line with the cine images due hardware setup limitations of the particular scanner [15-18]. The system is currently used as a virtual test-bed for designing and generating the appropriate control signals for a robotic manipulator (the latter being part of ongoing efforts [19]).

II. METHODOLOGY

The methodology is based on generating a time-dependent safe access trajectory for the robot to deploy through LV to the aortic annulus. In order to evaluate information that can be extracted from MR images and can be instrumental to plan and perform a transapical access to the beating heart, we investigated the specific MR slices that clearly show the LV in different planes. Fig. 2, on a long axis slice, depicts the trajectory which is to be updated on-the-fly as the procedure evolves, to reflect the morphologic changes in the beating heart [15, 19]. In order to construct 3D computational model of the

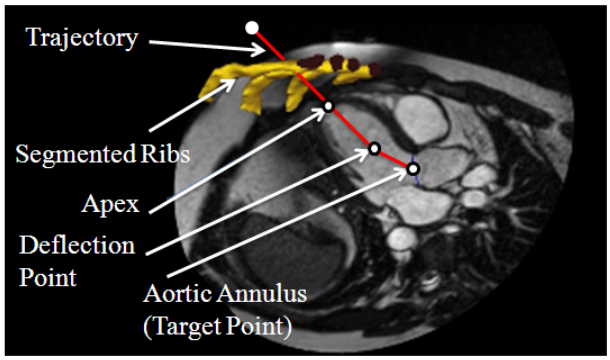

Fig. 2 Long axis slice shows the area of operation.

ribs, we performed manual segmentation of 2D MR images.

A. System Workflow

The system consists of three major components: dynamic sensing module (DSM), computational core, and human-machine interface (HMI) as shown in Fig. 3. For planning and robot control we used MRI datasets which were collected on healthy volunteers (n=10) with a true fast imaging, steady-state precession (TrueFISP) pulse sequence with the acquisition parameters: TR = 2.3 ms, TE = 1.4 ms, Alpha = 80°, slice thickness = 6 mm, interslice distance = 6 mm, and acquisition matrix = 224x256. Each data set included 24 slices (19 short and 5 long axes) each depicting the heart in 25 time frames. Those data were also used to assess the specific topography related to a transapical access to the aortic valve. Fig. 4 shows a long axis MR image of LV with the identified entrance point at the apex and targeted aortic valve annulus.

In a generalized transapical intervention scenario, a cardiologist (or surgeon) performs an anterolateral minithoracotomy of length 50-70 mm at the fifth intercostal space (the region between fourth and fifth ribs as depicted in Fig. 2) to directly access the apex of the heart and places a trocar with typical diameter of 15 mm on the tip of the apex to enter the left ventricle. As graphically illustrated in Fig. 4, the manipulator enters into the heart at the predefined apical point (P_A) and passes through LV toward the target point which is the center of the entrance of the aortic annulus (P_T). The manipulator is stabilized with controllable actuation, which provides a stable base for the subsequent steps of the procedure.

The robot must have enough maneuverability to reach safely from P_A to P_T in the dynamic environment of the beating heart. Standard cardiac anatomy (as also verified from multislice MRI of 10 different patients) suggests that in the general case, the deployment path of the manipulator from P_A to P_T is not a straight line. Indeed, a deflection point (P_D) near the base of the LV is needed. From the kinematic and path planning points of view, the major challenge is to determine the transient positions of P_A, P_D and P_T, which we termed as "guiding-points," and

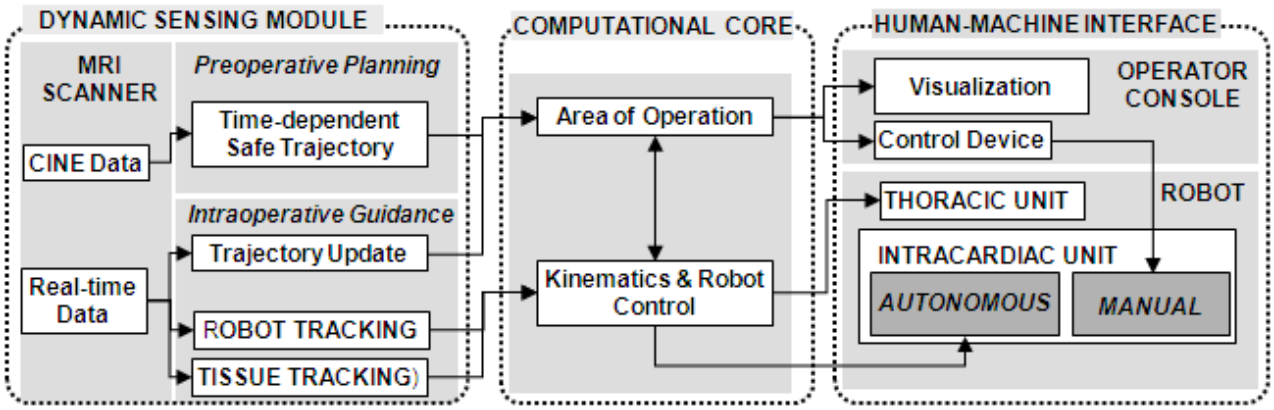

Fig. 3 Architecture of the proposed system and processes, delineating the three distinct synergizing components: sensing, computational core, and human-machine interface (including the robot).

a dynamic safe access corridor (S_C). Please note that, all MRI spatially-encoded information (e.g., coordinates) is taken with respect to the inherent, absolute coordinate system of the MR scanner.

Considering the current simulation and potential future applications, this work is built on top of the following assumptions. First, we determine the apical entrance point (P_A) from cine images, but in an *in vivo* scenario, appropriate MRI methods can provide the position of the trocar in RT (e.g., using miniature RF coil beacons on the robot [20]). Second, the access corridor S_C is extracted and updated from multislice cine MR Images that are appropriate for detailed dynamic 3D modeling of the LV and preoperative planning. Also, the long duration of acquiring a full cine set is not appropriate for intraoperative imaging. In practice, a single or a limited number of intraoblique slices can be used for fast imaging of the LV and update of the preimaged oblique slab(s) of the S_C (as reported previously [4, 5]). Third, the coordinates of the targeted point P_T can be extracted from the same limited number of slices with fast tissue tracking algorithms [18, 21]. Based on the above MR-extracted information, the deflection point P_D can then be safely identified as the intersection of the mid-annular line and the centerline of the access corridor S_C.

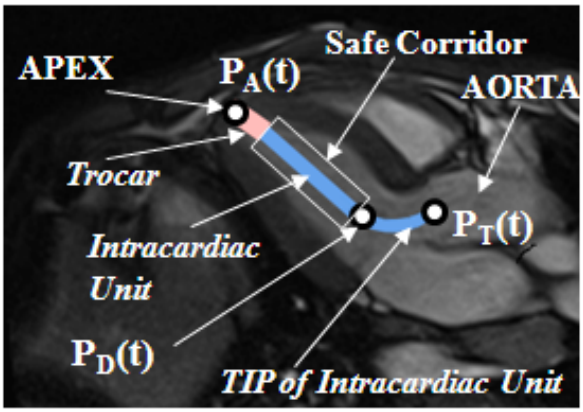

Fig. 4 Intracardiac unit of the manipulator enters the LV via a trocar with the diameter of 15mm. P_A, P_D, and P_T points are dynamically calculated during the process.

B. Dynamic Sensing Module

The major task of DSM is data processing which entails the detailed segmentation of the endocardium and the identification of the three guiding points: the apical (P_A), the mid-LV (P_D) and the target (P_T) at the center of the aortic annulus. The cine datasets of short axis (SA) and long axis (LA) images were segmented using our custom software endowed with Insight Toolkit (ITK) routines to extract the LV and the aortic annulus by tracing the corresponding endocardial boundary [16].

In order to create the safest access corridor in LV, we also considered the details of the papillary muscles in segmentation process. Indeed, the access corridor S_C must keep the robotic manipulator inside the blood-pool of the LV, without allowing it to touch the endocardium or the papillary muscles. Fig. 5 shows a sample segmentation of a short axis slice in the full-diastole phase of the heart. Please note that, the papillary muscles were also segmented out for a naturalistic extraction of the LV blood-pool.

As also reported in [16], the corridor creation algorithm performed three main steps for every time frame with a conservative approach to account for not-moving (akinetic) and partially-moving (dyskinetic) areas. First, all SA slices having visible blood-pool were determined by checking the inside surface areas of the segmented LV contours. Second, these contours were projected onto a virtual plane which is parallel to the SA slices, and their intersection was calculated. This projection was based on the fact that SA slices were parallel to each other and

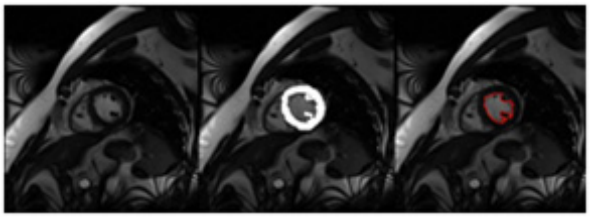

Fig. 5 Sample short axis slice showing full-diastole phase of the heart cycle. Second image depicts the segmentation result of ITK whereas the last one shows the endocardial boundary contour. The region inside of a boundary contour is the blood pool (inside of LV).

collected with the same field of view. Finally, this intersection (common area for all the slices) was linearly extruded from the apex to the base of the heart to form the volumetric corridor for that particular time frame (S_C (t), ∀t: t=1 to 25).

The pillar-like volumes in Fig. 6 depict these safe access corridors in different heart phases. The robot will not touch the inner walls of the left ventricle, including the papillary muscles, as long as it stays inside the corridor in every single time frame.

The coordinates of the apical point, P_A (t), for any time frame (t) were determined by identifying the extreme point of the apex on the central long axis view, which was further verified by assessing whether it belongs to a SA slice that does not depict any blood pool (i.e., it is only myocardium) for the time frame. The coordinates of the targeted point, P_T (t), were determined from the segmentation contours of two LA and one SA slices that included the aortic valve annulus at the level of the aortic valve leaflets, as the midline aortic annulus. In a real operation, a surgeon or a cardiologist can define the exact target point according to his/her personal surgical approach to AVI. The deflection point for any time frame, P_D (t), was then assigned as the intersection of the aortic annulus midline (known from the previous step) with the segmented contour of the first-to-cross SA slice. Finally, the extracted guiding points P_A (t), P_D (t) and P_T (t) were sent to the control module and the access corridor S_C (t) was sent to the visualization module.

C. Computational Core and Robot

This module determines the values of the DOFs of the robot for its deployment from the apical point (P_A) to the targeted point (P_T) via the deflection point (P_D), as well as for holding its position at any intermediate or terminal arrangement specified by the operator (Fig. 7). The inputs to this module are the dynamic coordinates of the aforementioned guiding-points P_A (t), P_D (t) and P_T (t) and the initial conditions specified by the operator: the time frame when the robot initiates its maneuvering, and whether and for how long it may hold a certain position along its path. The robotic manipulator was combined with the MR data to visualize the detailed operation.

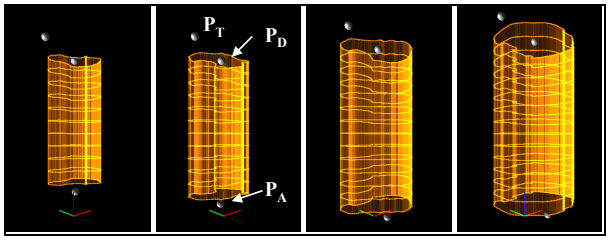

Fig. 6 Four selected frames (out of a total of 69) showing the access corridor and the three guiding-points which are calculated with respect to the MR scanner coordinate system and updated dynamically (25 time frames per heart-cycle).

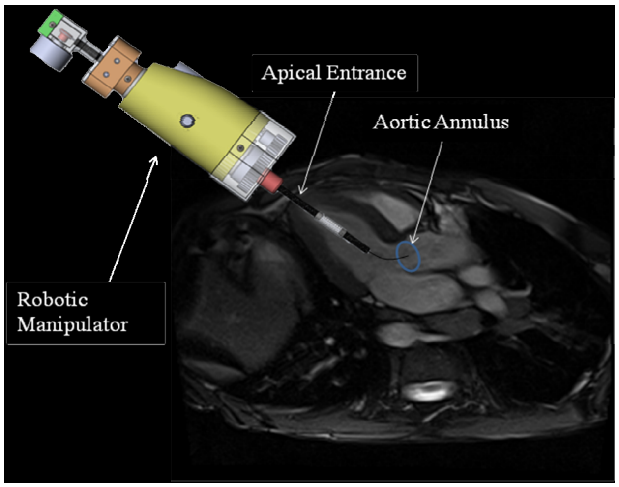

Fig. 7 Operational Scenario simulated with the manipulator inside the left ventricle (Shown in a long axis slice).

D. Visualization and HMI

The purpose of the visualization module is to generate and update a virtual reality environment that simulates the Area of the Procedure (AoP) which was implemented with OpenGL and GLUT libraries. The visualization module can display any combinations of the following objects: MR images, the segmentation contours, the three guiding points, the 3D access corridor, and the virtual robot. The AoP is built relative to the inherent coordinate system of the MR scanner, which offers a natural space of visualizing 3D geometric structures. The update rate of the AoP is the same as that of the collected MR images. In its basic form, the AoP can display and refresh the positions of the three guiding points.

The access corridor may also be included with or without the manipulator. When the robot is selected, its base appears anchored to the static or transient position of the apical point P_A. Different scenarios can be simulated to assess the beginning of a procedure, the idling of the manipulator at any instance, or the whole duration of the heart cycle (Fig. 8, 9).

Motion of the virtual robot entails the following three steps: deployment of the first link from the apex to the top of the LV point P_D, extension of the second link toward the targeted point P_T, and the holding of the position. During the maneuvering process, the control module supplies the values of the updated DOFs for each time instance. For the purpose of visualization, the intersections of P_A to P_D line with all the slices are calculated and depicted. The manipulator progressively moves along these intersections.

III. Results

In order to assess its feasibility, the system was tested using cine data for a number of simulation scenarios: different speeds of deployment (i.e., how many steps are performed per time frame), different heart phases when operation started, holding of the robot at a particular

configuration, and different number of simulated heart cycles. After an initial user-selected short idling period, there are two phases of robot maneuvering. The first one is the extension of the first link from the apical point P_A toward the deflection point P_D. In this phase, two rotational DOFs are actuated to maintain the deployed link inside the access corridor S_C and along the P_A to P_D line. After the distal end of the first link reaches the base point P_D, the second phase starts immediately and entails the extension of the second link to reach the targeted point P_T at the entrance of the aortic valve annulus. Once the annulus is reached, the robot maneuvering is performed to hold the position: the base of the robot at the apical point, the distal end of the first link at P_D, and the distal end of the second link at P_T. The same field of view was used in all frames and the panels were numbered from left to right and top to bottom accordingly.

Since there are 25 slices per full heart cycle, the update rate is approximately 35ms per frame. The whole image processing time including the corridor construction takes 10ms, which is less than the update rate. Further analysis of S_C showed that its average base area from 10 patients takes the minimum value of 97 mm^2 in systole and maximum value of 430 mm^2 in diastole, which is wide enough for the safe access of a robotic delivery device with diameter of up to 9 mm.

IV. DISCUSSION AND CONCLUSION

In this paper we described a novel computational system for modeling MRI-guided robot assisted interventions in the beating heart. The structure of the computational core has been designed scalable and modular in order to accommodate the additional functions planned to incorporate with future animal studies.

Although our methodology is proven to be adequate for implementing the backbone of the computational core, it has certain limitations currently with regard to the method used for tracking the guiding points. We used off-line cine images, rather than RT MRI as is the case in an *in vivo* experimental study. First, investigation of the system off-line was necessary with the setup of the particular MR scanner. Second, with online access, cine images can be substituted intraoperatively with RT MRI guidance using a few slices combined with parallel imaging, nontriggered and with free-breathing patients [6, 7]. Besides, using cine images does not negate the generality of the system's applicability and efficacy. Indeed, our preoperative planning methodology does not need RT data since it is quite possible to get MR images of several slices before the operation to determine the aortic annular diameter, coronary ostial anatomy, apical entrance point and the characteristics of the safe access corridor [16]. RT MRI is needed intraoperatively to update the trajectory and follow the operation.

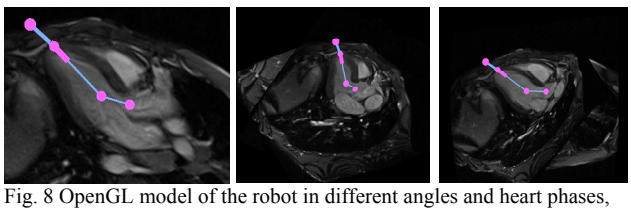

Fig. 8 OpenGL model of the robot in different angles and heart phases,

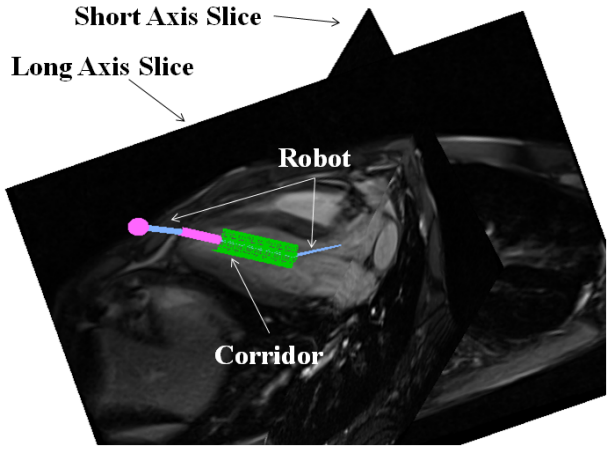

Fig. 9 OpenGL model of the robot in different angles and heart phases,

The robotic manipulator was modeled in the 3D CAD software SolidWorks based on the kinematic analyses we performed previously [16, 17]. In addition to intracardiac procedures, the manipulator can be further improved for performing other types of interventions within dynamically changing environments as well.

Our current work includes not only building the robotic manipulator physically for *in vitro* experiments, but also implementing an appropriate automatic segmentation algorithm [22], to directly interface the system with the MRI scanner in order to receive MR data as they are collected, and interactively control the image acquisition parameters on-the-fly [23].

REFERENCES

[1] F. A. Jolesz, "Future perspectives for intraoperative MRI," Neurosurg Clin N Am, vol. 16, pp. 201-13, Jan 2005.

[2] R. Mebarki, A. Krupa, and C. Collewet, "Automatic guidance of an ultrasound probe by visual servoing based on B-mode image moments," Med Image Comput Comput Assist Interv, vol. 11, pp. 339-46, 2008.

[3] S. G. Yuen, S. B. Kesner, N. V. Vasilyev, P. J. Del Nido, and R. D. Howe, "3D ultrasound-guided motion compensation system for beating heart mitral valve repair," Med Image Comput Comput Assist Interv, vol. 11, pp. 711-9, 2008.

[4] E. R. McVeigh, M. A. Guttman, R. J. Lederman, M. Li, O. Kocaturk, T. Hunt, S. Kozlov, and K. A. Horvath, "Real-time interactive MRI-guided cardiac surgery: aortic valve replacement using a direct apical approach," Magn Reson Med, vol. 56, pp. 958-64, Nov 2006.

[5] M. Li, D. Mazilu, and K. A. Horvath, "Robotic system for transapical aortic valve replacement with MRI guidance," Med Image Comput Comput Assist Interv, vol. 11, pp. 476-84, 2008.

[6] K. A. Horvath, D. Mazilu, M. Guttman, A. Zetts, T. Hunt, and M. Li, "Midterm results of transapical aortic valve replacement via real-time magnetic resonance imaging guidance," J Thorac Cardiovasc Surg, vol. 139, pp. 424-30, Feb.

[7] M. Li, D. Mazilu, B. J. Wood, K. A. Horvath, and A. Kapoor, "A robotic assistant system for cardiac interventions under MRI guidance," 2010, p. 76252X.

[8] K. S. Rhode, M. Sermesant, D. Brogan, S. Hegde, J. Hipwell, P. Lambiase, E. Rosenthal, C. Bucknall, S. A. Qureshi, J. S. Gill, R. Razavi, and D. L. G. Hill, "A system for real-time XMR guided cardiovascular intervention," Medical Imaging, IEEE Transactions on, vol. 24, pp. 1428-1440, 2005.

[9] A. C. Larson, R. D. White, G. Laub, E. R. McVeigh, D. Li, and O. P. Simonetti, "Self-gated cardiac cine MRI," Magn Reson Med, vol. 51, pp. 93-102, Jan 2004.

[10] S. Zhang, M. Uecker, D. Voit, K. D. Merboldt, and J. Frahm, "Real-time cardiovascular magnetic resonance at high temporal resolution: radial FLASH with nonlinear inverse reconstruction," J Cardiovasc Magn Reson, vol. 12, p. 39.

[11] M. Uecker, S. Zhang, D. Voit, A. Karaus, K. D. Merboldt, and J. Frahm, "Real-time MRI at a resolution of 20 ms," NMR Biomed, vol. 23, pp. 986-94, Oct.

[12] K. Cleary, A. Melzer, V. Watson, G. Kronreif, and D. Stoianovici, "Interventional robotic systems: applications and technology state-of-the-art," Minim Invasive Ther Allied Technol, vol. 15, pp. 101-13, 2006.

[13] M. Moche, R. Trampel, T. Kahn, and H. Busse, "Navigation concepts for MR image-guided interventions," J Magn Reson Imaging, vol. 27, pp. 276-91, Feb 2008.

[14] N. V. Tsekos, A. Khanicheh, E. Christoforou, and C. Mavroidis, "Magnetic resonance-compatible robotic and mechatronics systems for image-guided interventions and rehabilitation: a review study," Annu Rev Biomed Eng, vol. 9, pp. 351-87, 2007.

[15] E. Yeniaras, J. Lamaury, Z. Deng, and N. V. Tsekos, "Towards A New Cyber-Physical System for MRI-Guided and Robot-Assisted Cardiac Procedures," Proceedings of the 10th IEEE International Conference on Information Technology and Applications in Biomedicine, Nov,2010 2010.

[16] E. Yeniaras, Z. Deng, M. Davies, M. A. Syed, and N. V. Tsekos, "A Novel Virtual Reality Environment for Preoperative Planning and Simulation of Image Guided Intracardiac Surgeries with Robotic Manipulators," Medicine Meets Virtual Reality, vol. 18, p. To appear, 2011.

[17] N. V. Sternberg, Y. Hedayati, E. Yeniaras, C. E., and N. V. Tsekos, "Design of an actuated phantom to mimic the motion of cardiac landmarks for the study of image-guided intracardiac interventions," Proceedings of the 10th IEEE International Conference on Robotics and Biomimetrics, vol. 2010, 2010.

[18] Y. Zhou, E. Yeniaras, P. Tsiamyrtzis, N. Tsekos, and I. Pavlidis, "Collaborative Tracking for MRI-Guided Robotic Intervention on the Beating Heart," Proceedings of the 13th International Conference on Medical Image Computing and Computer Assisted Intervention (MICCAI), September,2010 2010.

[19] E. Yeniaras, N. Navkar, M. A. Syed, and N. V. Tsekos, "A Computational System for Performing Robot-assisted Cardiac Surgeries with MRI Guidance," in Proceedings of the 15th International Transformative Systems Conference, Dallas,USA, 2010, pp. 1-6.

[20] D. R. Elgort, E. Y. Wong, C. M. Hillenbrand, F. K. Wacker, J. S. Lewin, and J. L. Duerk, "Real-time catheter tracking and adaptive imaging," J Magn Reson Imaging, vol. 18, pp. 621-6, Nov 2003.

[21] Y. Zhou, P. Tsiamyrtzis, and I. Pavlidis, "Tissue Tracking in Thermo-physiological Imagery through Spatio-temporal Smoothing, ," in MICCAI, 2009, pp. 1092-1099.

[22] M. Fradkin, C. Ciofolo, B. Mory, G. Hautvast, and M. Breeuwer, "Comprehensive segmentation of cine cardiac MR images," Med Image Comput Comput Assist Interv, vol. 11, pp. 178-85, 2008.

[23] E. Christoforou, E. Akbudak, A. Ozcan, M. Karanikolas, and N. V. Tsekos, "Performance of interventions with manipulator-driven real-time MR guidance: implementation and initial in vitro tests," Magn Reson Imaging, vol. 25, pp. 69-77, Jan 2007.